Neutron Star Astrophysics at the Crossroads: Magnetars and the Multimessenger Revolution
Proceedings IAU Symposium No. 363, 2023
E. Troja & M. G. Baring, eds.
doi:10.1017/S1743921322000266

The new magnetar SGR J1830−0645 in outburst

Francesco Coti Zelati[1,2]

[1]Institute of Space Sciences (ICE, CSIC), Campus UAB,
Carrer de Can Magrans s/n, E-08193, Barcelona, Spain
email: cotizelati@ice.csic.es

[2]Institut d'Estudis Espacials de Catalunya (IEEC),
Carrer Gran Capità 2–4, E-08034 Barcelona, Spain

Abstract. The magnetar SGR J1830−0645 was discovered in outburst in October 2020. We studied its X-ray properties during the first month of the outburst using *XMM–Newton*, *NuSTAR* and *Swift* observations. The shape and amplitude of the pulse profile varied significantly with energy. The broadband spectrum was well described using two absorbed blackbody components plus a faint power law component at high energies. Phase-resolved spectral analysis of the data suggests that the emission could be attributed to thermal photons from a single heated region with a complex shape on the star surface undergoing resonant Compton scattering on charged particles located in the magnetosphere. Modelling the evolutionary path of the magnetar with our magneto-thermal evolutionary codes indicates that SGR J1830 was born ≈23 kyr ago with a dipolar magnetic field of $\sim 10^{15}$ G, slightly larger than the current value.

Keywords. stars: magnetic fields, (stars:) pulsars: general, X-rays: stars, X-rays: bursts.

1. Introduction

Magnetars are isolated pulsars with X-ray luminosities in the range $L_X \sim 10^{31}$–$10^{35}\,\mathrm{erg\,s^{-1}}$ whose emission is believed to be powered by the dissipation of their huge magnetic fields, $B \sim 10^{13} - 10^{15}$ G (Kaspi & Beloborodov 2018; Esposito et al. 2021). They are observed to emit bursts of X-rays on timescales from tens of ms up to hundreds of seconds (in three cases only), reaching peak luminosities in the range $L_X \sim 10^{38} - 10^{46}\,\mathrm{erg\,s^{-1}}$. These bursts often herald the onset of an X-ray outburst, a long-lasting transient episode where the X-ray luminosity increases by orders of magnitude and usually returns to the quiescent level on a timescale of months or even years (Coti Zelati et al. 2018).

SGR J1830−0645 (SGR J1830) is the penultimate addition to the magnetar family. It was discovered as it emitted a single-peaked, 6 ms-long burst of hard X-rays detected by *Swift* BAT on 2020 October 10. Subsequent observations in the soft X-ray band led to an accurate localization of the X-ray counterpart of the burst and to the detection of coherent X-ray pulsations from the source position at a period of about 10.4 s (see Coti Zelati et al. 2021 and references therein).

2. The X-ray properties of SGR J1830−0645 early in the outburst

We started an extensive follow-up X-ray monitoring campaign of SGR J1830 using quasi-simultaneous *XMM–Newton* and *NuSTAR* observations just three days after the discovery burst and high-cadence *Swift* observations along the first month of the outburst.

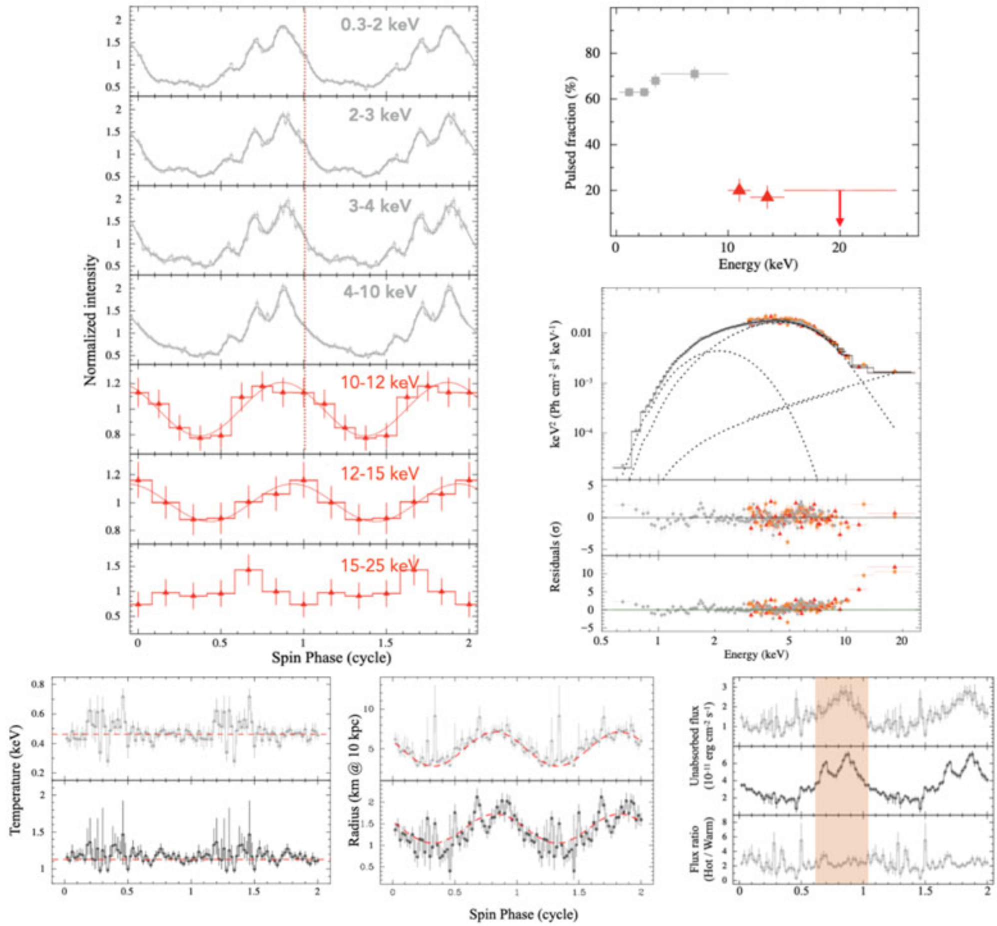

Figure 1. TOP: Pulse profiles (*left*) and pulsed fractions (*right*) of SGR J1830 in different energy bands. *Right, bottom*: Unfolded broadband spectrum of SGR J1830. The black solid line marks the best-fitting double blackbody plus power-law model, the dotted lines mark the contribution of the single spectral components. Best-fitting parameters are: $kT_1 = 0.45 \pm 0.01$ keV, $kT_2 = 1.11 \pm 0.01$ keV, $R_1 = 5.6 \pm 0.3$ km, $R_2 = 1.53 \pm 0.03$ km, $\Gamma = 0.9 \pm 0.3$. The middle panel shows the post-fit residuals, the bottom panel shows the residuals after removing the power-law component from the model. In all panels, light gray marks *XMM–Newton* EPIC-pn data, red *NuSTAR* FPMA and orange *NuSTAR* FPMB. BOTTOM: Evolution of the temperature (*left*), radius (*middle*) and unabsorbed fluxes (*right*) along the phase for the warm (light gray) and hot (dark grey) blackbody components. The unabsorbed flux ratio between the hot and the warm components is shown in the right bottom panel. The red dashed lines represent the best-fitting model using a constant term for the evolution of the temperatures (*left panel*) and a sinusoidal function with period fixed to the fundamental component of the pulsed signal for the evolution of the radii (*middle panel*). The red shaded area in the *right panel* marks the phase interval corresponding to the maximum values of the unabsorbed fluxes for both spectral components.

At the peak of the outburst, the pulse profile evolved from a multi-peaked morphology at energies below 10 keV to an almost sinusoidal shape at higher energies up to ≈15 keV. This remarkable change in the shape of the pulse profile was accompanied by a dramatic reduction of the pulsed fraction, from 60–70% at low energies down to 15–20% at higher energies (Fig. 1). The broadband average spectrum was well described by an absorbed double-blackbody model plus a power-law component over the 0.3–25 keV energy band (Fig. 1), giving an unabsorbed flux of $\sim 5.5 \times 10^{-11}$ erg cm^{-2} s^{-1}. The power-law

https://doi.org/10.1017/S1743921322000266 Published online by Cambridge University Press

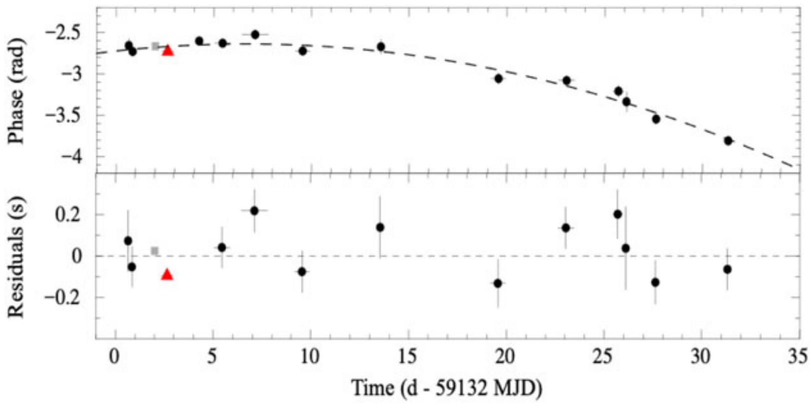

Figure 2. Phase evolution as a function of time of SGR J1830 fitted with a linear plus a quadratic components (upper panel). The residuals with respect to our best phase-coherent solution are reported in the lower panel, in units of seconds. Black circle, gray squares and red triangles points mark the *Swift* *XMM–Newton* and *NuSTAR* observations, respectively.

component contributed only $\simeq$6% to the overall flux and began to dominate over the thermal components only at energies above $\approx$12 keV, that is, at energies where the shape of the pulse profile became much simpler and its amplitude reduced considerably.

Fifty phase-resolved spectra were extracted using the *XMM–Newton* EPIC-pn data, and were modelled using an absorbed double-blackbody model. We found that, for both spectral components, the blackbody temperature remained fairly constant along the rotational phase, while the blackbody radius showed a clear modulation at the spin period that was rather smooth for the warm component and more complex for the hot component. This is also reflected in the period-folded flux light curves of both spectral components, where the light-curve profile associated with the hotter blackbody seemed to more closely track the fine structures seen in the low-energy pulse profiles. Both light-curve profiles were also well aligned in phase (Fig. 1).

Our extensive X-ray monitoring campaign using *Swift* XRT (14 observations over a 34-day baseline) has allowed us to extract a phase-connected timing solution using a phase-fitting technique (Fig. 2) and to measure the spin period derivative, $\dot{P} \sim 7 \times 10^{-12}\,\mathrm{s\,s^{-1}}$ hence a dipolar magnetic field at the pole of $B_{\mathrm{dip,p}} \approx 5.5 \times 10^{14}$ G, a spin-down luminosity of $L_{\mathrm{sd}} \approx 2.4 \times 10^{32}\,\mathrm{erg\,s^{-1}}$ and a characteristic age of $\tau \approx 24$ kyr. The unabsorbed X-ray flux of SGR J1830 decreased to $\sim 2 \times 10^{-11}\,\mathrm{erg\,cm^{-2}\,s^{-1}}$ after one month, that is, a factor of >15 above the flux limit derived from pre-outburst ROSAT observations of the field.

3. Discussion

The results of our analysis are consistent with a scenario in which the outburst of SGR J1830 was caused by the formation of a single heated region on the neutron star surface with a complex shape and a non-uniform temperature distribution. This interpretation is supported by recent 3D simulations that have shown how anisotropic heat propagation from a localized region in the crust to the surface can create complex hot spots on magnetar surfaces (De Grandis et al. 2020). Soft, thermal photons coming from such a spot are expected to produce a complex pulse profile with a high pulsed fraction (Albano et al. 2010). The decrease of the pulsed fraction at higher energies is compatible with a scenario where resonant Compton scattering of thermal photons on charged particles in the magnetosphere acts in the direction of smearing out the (pulsed) thermal emission, possibly due to a peculiar location and/or velocity distribution of the charges.

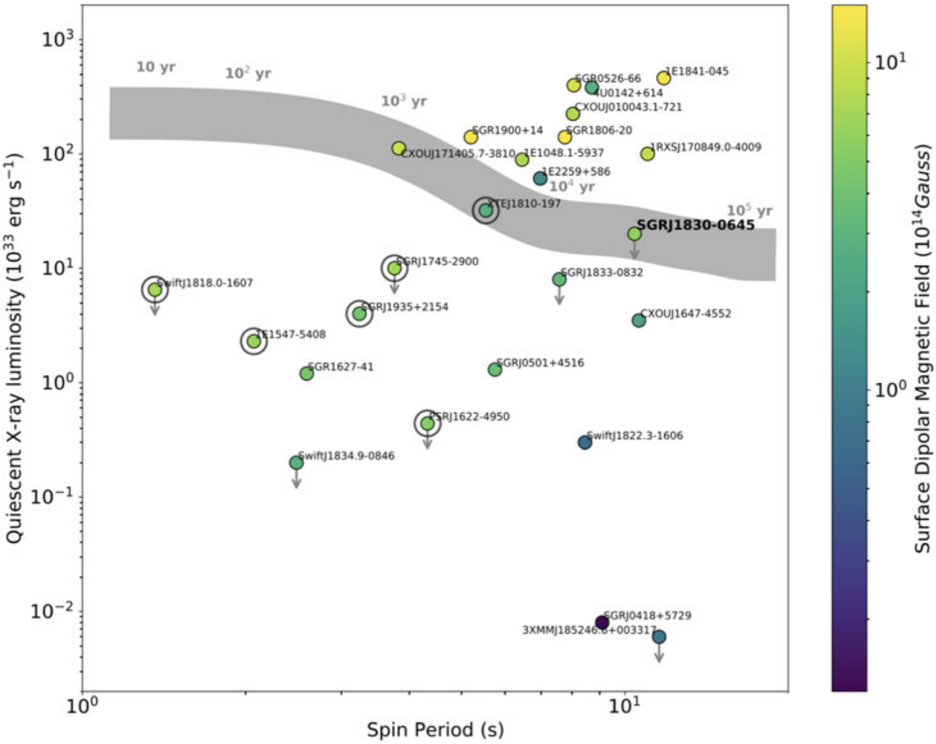

Figure 3. Quiescent X-ray luminosity as a function of the spin period for magnetars, including SGR J1830 (in bold). Circles mark radio-loud magnetars. The gray shaded region shows the magneto-thermal evolutionary path of SGR J1830 according to our model.

We have studied the evolutionary history of SGR J1830 using a 2D magneto-thermal evolutionary code (see Viganò et al. 2021 and references therein) and crustal-confined models consisting of an initial magnetic field with equal amounts of energy in the poloidal and toroidal components. The current spin parameters of SGR J1830 can be reproduced by letting an initial dipolar magnetic field of $B_{\rm dip,in} \approx 10^{15}$ G evolve for $\approx$23 kyr (see the gray shaded region of Fig. 3 for the evolution of the spin period and luminosity of SGR J1830 according to our codes compared to the current values for other magnetars). The similarity of this value with the timing-inferred characteristic age is not so surprising, since the magnetic field dissipation is not yet substantial at this evolutionary stage.

Future X-ray observations will be crucial in mapping the evolution of the heated spot of SGR J1830 to improve our understanding of the surface emission from this and other magnetars (see Younes et al. 2022 for a recent study), as well as in assessing the long-term contribution of magnetospheric currents to the X-ray emission of SGR J1830.

References

Albano, A., Turolla, R., Israel, G. L., et al. 2010, *ApJ*, 722, 788
Coti Zelati, F., Rea, N., Pons, J. A., et al. 2018, *MNRAS*, 474, 961
Coti Zelati, F., Borghese, A., Israel, G. L., et al. 2021, *ApJ* (Letters), 907, L34
De Grandis, D., Turolla, R., Wood, T. S., et al. 2020, *ApJ*, 903, 40
Esposito, P., Rea, N., & Israel, G. L. 2021, Astrophysics and Space Science Library, 461, 97
Kaspi, V. M. & Beloborodov, A. M. 2017, *ARAA*, 55, 261
Viganò, D., Garcia-Garcia, A., Pons, J. A., et al. 2021, Computer Physics Communications, 265, 108001
Younes, G., Lander, S. K., Baring, M. G., et al. 2022, *ApJ* (Letters), 924, L27